Moisture Content Distribution in Semibatch Drying Processes. I. Constant Particle Drying Rate

Bernardus J. Nitert and Michael J. Hounslow
Dept. of Chemical and Biological Engineering, The University of Sheffield, Shefield S1 3JD, UK

DOI 10.1002/aic.13791
Published online April 4, 2012 in Wiley Online Library (wileyonlinelibrary.com).

*Semibatch drying processes include a period of feeding wet particles during drying. This results in different residence times of particles in the dryer and thus generation of a moisture content distribution. Describing these processes in a model that takes this moisture content distribution into account can be complicated. Knowledge of minimum or maximum values of the moisture content distribution is often desired for subsequent process steps or end product quality. This article presents a model that not only describes the overall average moisture content in time during semibatch drying put also gives the evolution of the moisture content distribution in time. A novel solution strategy based on the "*method of moments*" and "*method of characteristics*" is presented that solves the resulting ordinary differential equations in a piecewise manner. Simulations for a semibatch fluidized bed drying process give results that are feasible and realistic.* © 2012 American Institute of Chemical Engineers *AIChE J,* 58: 3697–3707, 2012
Keywords: design (process simulation), drying, mathematical modeling, particle technologh, simulation, process, population balance model

Introduction

Particle-size enlargement is often performed by spraying binder onto primary particles. In most cases, this binder consists of solvent and optionally a compound that promotes binding between particles. Excess solvent has to be removed, as it will cause powder handling problems later in the manufacturing process (e.g., powder flow from a hopper). Another application of a drying operation is removal of abundant solvent from filtered crystals. Different drying techniques are available for solvent removal. It depends on the particle size and nature of feed which technique is preferred.[1] A fluidized bed is often used, as it provides high thermal efficiency and drying intensity because of high heat and mass transfer rates. Many authors have modeled fluidized bed drying for example, Ref. 1–5. Others have restricted their work to heat transfer in gas–solid systems.[6–8] It is beyond the scope of this article to discuss this work. Most important is to recognize that implementation of population dynamics in the model improves its accuracy.[9] Burgschweiger and Tsotsas[2] have developed a very thorough and extensive model for continuous fluidized bed drying systems by defining a residence time density distribution for particles in the dryer. This distribution is coupled to moisture content, mass, and enthalpy balances. A solution strategy based on the method of characteristics is applied. Unfortunately, all physical process parameters have to be known to solve the coupled balance equations. For a continuous process in steady state, the moisture content distribution resulting from a residence time distribution is not changing in time, which is probably why the author only presented average values for moisture content and temperature in his simulations. Metzger et al.[9] concluded that existing drying models still build on average values for moisture content, and it is desired to find new modeling approaches to include moisture content distributions in population balances. Peglow et al.[10] have presented a simple population balance model also on the basis of residence time distribution. A moisture content distribution for continuous fluidized bed drying during steady state was calculated. However, semibatch drying processes are constantly in a nonsteady state, that is, the moisture content distribution is constantly changing in time. From an industrial point of view, it is interesting to know how it changes in time, as measures can be taken to prevent single particles becoming too wet or too dry.

This article presents a model that describes the evolution of moisture content distribution in time for semibatch drying processes. First, definitions for constant and falling drying rate are given. These drying rates are then coupled to population balance equations that can b e solved numerically using a novel solution strategy. Finally simulations are performed using semibatch fluidized bed drying as an example. The ultimate goal of applying this model in industrial processes is faster development of drying processes that are more efficient in process time as well as energy consumption.

Defining the Drying System

In an arbitrary drying system, two environments can be distinguished: (1) a microenvironment that describes drying of a single particle in the system and (2) a macroenvironment that describes drying of all particles in the system. In

Correspondence concerning this article should be addressed to M. J. Hounslow at m.j.hounslow@sheffield.ac.uk.

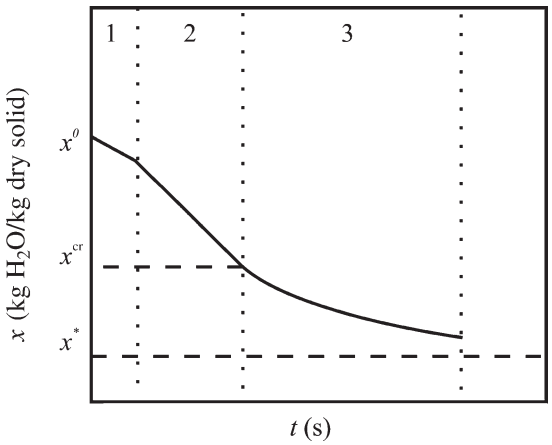

Figure 1. Characteristic drying curve for a single particle.

Stage 1 represents the initial stage where $T < T_s$. Constant rate drying ($x \geq x^{cr}$) is stage 2 (dx/dt is independent of x). Stage 3 ($x < x^{cr}$) illustrates falling rate drying (dx/dt is depending on x).

the following subsections, definitions for constant and falling drying rates are presented for both environments.

Single particle drying rate

In this article, (particle) drying rate is defined as the reduction of (particle) moisture content per unit of time ($\dot{x}(x|t)(= dx/dt)$ in kg solvent kg dry solid^{-1} s^{-1}). This rate should be regarded differently from the definition of "flux" where change of exchange surface area is also taken into account. Three stages can be distinguished (see Figure 1)[11]:

1. *Initial stage*: particle surface is covered with liquid of lower temperature than the equilibrium temperature*. This stage is often considered to have a negligible effect on the drying rate.

2. *Constant drying rate*: the drying rate is independent of x and constant in time. It is determined by external drying conditions (T_g, u_g, Y_g), until the moisture content x has reached a critical value x^{cr}. This value is the point where the particle surface is no longer fully covered with liquid to evaporate.

3. *Falling drying rate*: when $x < x^{cr}$, the drying rate depends on x and is determined by (internal) parameters that influence internal diffusion to the particle surface (e.g., innerparticle porosity and tortuosity).

For the stages of constant and falling drying rate, the following definitions for dx/dt are applicable:

Constant drying rate

$$dx/dt = \dot{x}(x|t) = -k(t) \tag{1}$$

Falling drying rate

$$dx/dt = \dot{x}(x|t) = -k(t)(x - x^*)/(x^0 - x^*) \tag{2}$$

where $k(t)$ is a proportionality constant describing the slope of the (x, t)-plot. where "|" separates dependent (left) and independent (right) variables.

Overall drying rate in system

In the previous section, constant and falling drying rates were defined for single particles. Although these drying rates indirectly determine the overall drying rate of the system, it is more convenient to use the mass balance of solvent in the drying system to define the overall constant and falling drying rate. Solvent is removed from the system at a net rate of χ (in kg/s). In semibatch and continuous drying systems, solvent enters the dryer in the form of wet particles at a rate w^0x^0 (see Figure 2). The following definitions apply to these systems:

Constant drying rate

$$\chi = \text{constant}$$

Falling drying rate

$$\chi = \gamma(t)\frac{\bar{x}_{\text{overall}} - x^*}{x^0 - x^*}$$

where for falling drying rate, χ is a function of the average overall drying rate $\bar{x}_{\text{overall}}$ in the system and $\gamma(t)$, a proportionality constant describing the dependence of $\bar{x}_{\text{overall}}$ as a function of time. The definition of constant drying rate is valid when

1. All wet particles in the system together release the same absolute amount of solvent per unit of time (kg/s).

2. Regardless of the state of different particles, the outgoing airstream of the dryer is saturated with solvent vapor (deep bed drying). In other words, the total amount of solvent extracted from particles present in the dryer is constant when inlet air conditions, also remain constant.

Similar to single particle drying, overall constant drying rate is also followed by falling drying rate. This occurs when the average overall moisture content $\bar{x}_{\text{overall}}$ has reached a critical value $\bar{x}^{cr}_{\text{overall}}$. Continued drying results in a lower overall transportation rate of solvent from particles to the bulk gas in comparison with the overall removal rate of solvent ($d\bar{x}_{\text{overall}}/dt < -\chi$). The outgoing airstream is no longer saturated with solvent vapor.

It is emphasized that although a macrosystem with saturated outgoing airstream is in a state of constant drying rate (χ = constant and $\bar{x} > \bar{x}^{cr}$), it is possible for individual particles to have reached the stage of falling drying rate ($\dot{x}(x|t) = -k(t)(x - x^*)/(x^0 - x^*)$). However, their contribution is not sufficient enough to result in an unsaturated outgoing airstream.

A semibatch drying system

In this article, the following assumptions are made regarding single and overall drying rate

Constant particle drying rate: $dx/dt = \dot{x}(t)$.

Constant overall solvent removal rate: χ = constant.

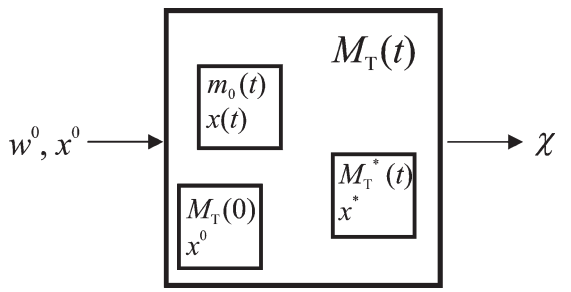

Figure 2. Schematic overview of an arbitrary drying system.

The arrows indicate the feed rate w^0 of wet particles with moisture content x^0 (left arrow) and net overall solvent removal rate χ (right arrow). At a time t, the dryer contains $M_T(t)$ kg particles that consists of $m_0(t)$ kg wet particles and $M_T^*(t)$ dry particles (masses on basis of dry solid). $M_T(0)$ represents the initial charge.

*Equilibrium temperature or wet bulb temperature is the temperature at which the heat transmitted to the surface equals the heat required for moisture evaporation.

These assumptions have been made for the purpose of obtaining an analytical solution of the population balance equations. It has to be emphasized that their validity in real systems can be questioned. As discussed later, it is recommended to investigate this in practice.

Figure 2 shows a schematic overview of a semibatch drying process. The dryer is fed with wet particles of moisture content x^0 and feed rate w^0. An initial charge is added to obtain a constant χ during the entire drying process, that is, including $t = 0$. When no initial charge is added, $\chi = 0$ at $t = 0$ as there is no material to dry. At some point in time, the dryer contains a mass $M_T(t)$ of particles on a dry basis which must equal the mass charged, at a rate w^0, plus the initial charge $M_T(0)$

$$M_T(t) = \int_0^t w^0\, dt + M_T(0) \tag{3}$$

The Model

For a semibatch drying process, it is trivial to define a population balance that describes the evolution of moisture content (distribution) in time. Contrary to a batch process, residence times of particles in the dryer are different, that is, they do not contain the same moisture content during the process. Instead, a distribution of moisture contents is obtained.

This section presents a population balance model and solution strategy based on the ''method of characteristics'' and ''method of moments'' for evolution of the moisture content distribution in time. In addition to the assumptions for drying rates, the following assumptions are also made:

- Particles do not aggregate, attrit, or break during the process.
- x^* is independent of time.
- Particles are not removed by filters or adhesion to walls.
- The particles are well mixed in the drying system.
- The drying rate of a single particle depends only on the moisture content of that particle and the local air humidity.
- Feed moisture content x^0 and feed rate w^0 are constant during feeding.
- No shrinkage of particles during solvent removal.

For a collection of particles with moisture contents $x \in (x^0, x^*)$ in the dryer, the following mass density function with moisture content x as the internal coordinate and bed length y as external coordinate can be written

$$f_{tot}(x|y,t) = f(x|y,t) + M_T^*(t)\delta(x - x^*) \tag{4}$$

Equation 4 shows that the total moisture content distribution $f_{tot}(x|y,\ t)$ is divided into a wet particle distribution, $f(x|y,t)$, and a dry particle population of $M_T{}^*(t)$ kg of dry particles with moisture content x^*. This distinction is made as not all particles reach the equilibrium moisture content x^* at the same time contrary to the batch system described above in which they do. $M_T{}^*(t)$ can be calculated from the mass balance

$$M_T^*(t) = M_T(t) - m_0(t) \tag{5}$$

where $m_0(t)$ is the mass of wet particles and will be explained in more detail later. When particles have reached x^*, they join the dry particle population $M_T^*(t)$. All particles with moisture content $x > x^*$ are part of the wet particle population $f(x|y,\ t)$. Ultimately, all particles will join $M_T^*(t)$. The mass of particles with $x \in (x,\ x + dx)$ can be obtained by integrating $f_{tot}(x|y,\ t)$ over x: $dM_T = f_{tot}(x|y,\ t)dx$. All masses are expressed on the basis of dry solid.

In what follows, we:

- show that the population balance is not a function of bed length y.
- develop equations for the corresponding moments and subsequently average properties of the system.

Defining a population balance for wet particle population

For a collection of wet particles in the dryer, $f(x|y,\ t)$, the following population balance is defined

$$\frac{\partial f(x|y,t)}{\partial t} + \frac{\partial (f(x|y,t)u_y)}{\partial y} + \frac{\partial (f(x|y,t)\dot{x}(x|y,t))}{\partial x} = w^0\delta(x - x^0)\delta(y - y^0) \tag{6}$$

Spatial averaging over bed length y is performed as a well-mixed bed and deep bed drying are assumed. First, the mass density function of wet particles $f(x|y,\ t)$ is normalized over the total bed length y_{bed}.

$$f(x|y,t) = \frac{f(x|t)}{y_{bed}} \tag{7}$$

In this article, constant particle drying rate is assumed, giving the following expression for $\dot{x}(y,t)$[11]

$$\dot{x}(y,t) = k''(t)(Y_w - Y_g(y)) \tag{8}$$

When applying the same spatial averaging over bed length y to Eq. 8, the following expression is obtained

$$\dot{x}(y,t) = \int_0^{y_{bed}} \frac{k''(t)(Y_w - Y_g(y))}{y_{bed}}\, dy \tag{9}$$

Deep bed drying is assumed, which means that the outgoing air is always saturated with moisture. This assumption is only valid when inlet ($Y_g(0)$) and outlet ($Y_g(y_{bed})$) moisture content of the air are constant. As a result, $\dot{x}(y,t)$ is independent of the position of particles in the bed, when deep bed drying is assumed. The latter meaning that

$$\dot{x}(t) = k'(t) \tag{10}$$

Incorporating Eqs. 7 and 8 into Eq. 6 and integrating over y gives

$$\frac{\partial f(x|t)}{\partial t} + \left[f(x|y,t)u_y\right]_0^{y_{bed}} + \dot{x}(t)\frac{\partial f(x|t)}{\partial x} = w^0\delta(x - x^0) \tag{11}$$

As there is no flux of particles in the y-direction: $u_y = 0$. This reduces Eq. 11 to

$$\frac{\partial f(x|t)}{\partial t} + \dot{x}(t)\frac{\partial f(x|t)}{\partial x} = w^0\delta(x - x^0) \tag{12}$$

where $f(0|t) = 0$ and $f(x|0) = M_T(0)\delta(x - x^0)$.

Calculation of overall average moisture content

Many drying processes are evaluated based on their overall average moisture content. This parameter is calculated

from Eq. 12 using the method of moments. As described in the previous section, the total mass of wet particles is obtained from the zeroth moment of $f(x|t)$. The first moment of $f(x|t)$ gives the total mass of solvent in wet particles as a function of time

$$m_0(t) = \int_{x^*}^{x^0} f(x|t)\,dx \tag{13}$$

$$m_1(t) = \int_{x^*}^{x^0} xf(x|t)\,dx \tag{14}$$

The average moisture content of wet particles as a function of time is calculated with

$$\bar{x}(t) = \frac{m_1(t)}{m_0(t)} \tag{15}$$

In practice, it is more useful to know the overall average moisture content, that is, including dry particles. The fraction of dry particles is calculated using the fraction of wet particles ($m_0(t)/M_T(t)$). The fraction of dry particles becomes

$$P_{\text{dry}}(t) = 1 - \frac{m_0(t)}{M_T(t)} \tag{16}$$

The overall average moisture content ($\bar{x}_{\text{overall}}(t)$) is obtained from

$$\bar{x}_{\text{overall}}(t) = P_{\text{dry}}(t) \cdot x^* + (1 - P_{\text{dry}}(t)) \cdot \bar{x}(t) \tag{17}$$

Defining a dimensionless population balance equation

The previous section showed that the zeroth and first moment of $f(x|t)$ are used to calculate the evolution of overall average moisture content in time. However, this requires information about $f(x|t)$, that is, moisture content distribution within a population of wet particles. In practice, this information is not available, as it would require measurement of the moisture content of each individual particle. In most cases, the only available data are initial particle moisture content, x^0, final particle moisture content, x^*, inlet mass flow, w^0, drying rate, χ, total batch size, and initial mass in dryer, $M_T(0)$. Successful solution of the PBE (Eq. 6) with these input parameters is achieved by finding an expression that couples them to the PBE. Such an expression is found by first converting the mass density function, $f(x|t)$, into a dimensionless density function, $g(z|\theta)$, where z is the dimensionless dryness defined by

$$z(x) = \frac{x - x^0}{x^* - x^0} \tag{18}$$

and θ is a dimensionless time or extent of drying defined by

$$d\theta = \dot{z}(t)dt \quad (\text{with } d\theta/dz = 1) \tag{19}$$

where $\dot{z}(t)$ is the dimensionless drying rate calculated from the nondimensionless drying rate ($\dot{x}(t)$) using the chain rule $\dot{x}(t)$ is obtained from χ and $f(x|t)$

$$\chi = -\int_{x^*}^{x^0} \dot{x}(t) f(x|t)\,dx \tag{20a}$$

$$\dot{x}(t) = -\frac{\chi}{m_0(t)} \tag{20b}$$

In a semibatch process $m_0(t)$ is changing with time. With χ being constant, this also means that $\dot{x}(t)$ is changing in time, until all particles are fed to the dryer (see Eq. 20b). Nevertheless, $\dot{x}(t)$ is still independent of x.

Eq. 18 gives

$$\frac{dz}{dx} = \frac{1}{x^* - x^0}$$
$$\dot{z}(t) = \frac{\chi}{m_0(t)(x^0 - x^*)} \tag{21}$$

The dimensionless dryness (z) is used to define a new pdf, $g(z|\theta)$

$$g(z|\theta)|dz| = \frac{1}{M_T(0)} f(x|t)|dx| \tag{22}$$

$$g(z|\theta) = \frac{x^0 - x^*}{M_T(0)} f(x|t) \tag{23}$$

Substituting Eqs. 19 and 23 into Eq. 6 gives

$$\frac{\partial g(z|\theta)}{\partial \theta} + \frac{\partial g(z|\theta)}{\partial z} = \alpha(\theta)\mu_0(\theta)\delta(z) \tag{24}$$

with

$$\alpha = \frac{(x^0 - x^*)w^0}{\chi} \tag{25}$$

and $\mu_0(\theta)$, which is the dimensionless mass of wet particles in the dryer

$$\mu_0(\theta) = \int_0^1 g(z|\theta)dz \tag{26}$$

$$= \frac{m_0(t)}{M_T(0)} \tag{27}$$

Also $\mu_1(\theta)$ is defined representing the dimensionless mass of dryness among wet particles

$$\mu_1(\theta) = \int_0^1 zg(z|\theta)dz \tag{28}$$

From Eqs. 26 and 28, the overall dimensionless dryness among wet particles in the dryer can be calculated

$$\bar{z}(\theta) = \frac{\mu_1(\theta)}{\mu_0(\theta)} \tag{29}$$

The overall dimensionless wetness, $1 - z$, can also be expressed in terms of $\mu_0(\theta)$ and $\mu_1(\theta)$

$$\int_0^z (1 - z)g(z|\theta)\,dz = \mu_0(\theta) - \mu_1(\theta) \tag{30}$$

The change of dimensionless wetness in θ is then calculated with the following Ordinary differential equation (ODE) when α is constant during each feeding phase (i.e., constant χ and constant w^0)

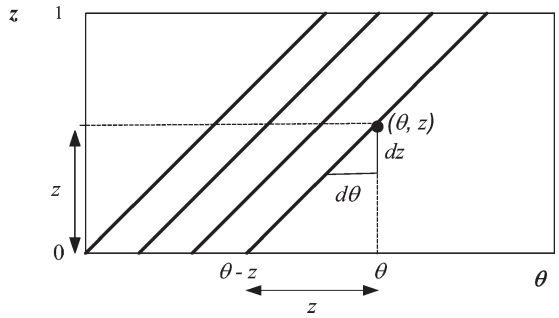

Figure 3. Method of characteristics for $g(z|\theta)$ ($dz/d\theta = 1$). $g(z|\theta)$ does not change along a characteristic, that is, $g(z|\theta) = g(0|\theta - z)$.

This insight is exploited to find expressions for $\mu_0(\theta)$ and $\mu_1(\theta)$ that are used to find $g(z|\theta)$ and $f(x|t)$.

$$\frac{d(\mu_0(\theta) - \mu_1(\theta))}{d\theta} = (\alpha(\theta) - 1)\mu_0(\theta) \tag{31}$$

Finding expressions for $\mu_0(\theta)$ and $\mu_1(\theta)$

The population balance of $g(z|\theta)$ (Eq. 24) cannot be solved without knowing $\mu_0(\theta)$. Equation 26 shows that $g(z|\theta)$ as a function of z is required to find $\mu_0(\theta)$. A solution has to be found that gives an expression for $\mu_0(\theta)$ independent of $g(z|\theta)$. The method of characteristics provides an excellent way to find such an expression. A collection of wet particles start a characteristic at $z = 0$ and dimensionless time θ. They leave the wet particle population at $z = 1$. For $z > 0$, the following condition applies for Eq. 24: $Dg/D\theta = 0$. This means that along a characteristic $g(z|\theta)$ does not change. Figure 3 shows that, with $dz/d\theta = 1$, the following condition applies for any point (θ, z) on a characteristic

$$g(z|\theta) = g(0|(\theta - z)) \tag{32}$$

Substituting Eq. 32 into the population balance (Eq. 24) gives

$$g(0|(\theta - z)) = \alpha(\theta - z)\mu_0(\theta - z) \tag{33}$$

This powerful insight is used to obtain expressions for $\mu_0(\theta)$ and $\mu_1(\theta)$ without knowledge of $g(z|\theta)$. The start of every characteristic is defined v and is equal to $\theta - z$. This definition is incorporated into Eq. 33. When a collection of wet particles enter the dryer and start a characteristic at $v = \theta - 1$, these particles will be fully dry at θ, that is, when $z = 1$. The boundary conditions in Eqs. 26 and 28 of $z = 0$ and $z = 1$ are, respectively, $v = \theta - 1$ and $v = \theta$. However, it is important to recognize that there is a discontinuity at $\theta = 1$. Here, the initial charge, $M_T(0)$, leaves the wet particle population to join the dry particle population, $M_T{*}(t)$. In other words, up to $\theta = 1$ the initial charge has to be included in expressions for $\mu_0(\theta)$ and $\mu_1(\theta)$ while from $\theta = 1$ onward, the wet particle population only consists of particles that have been fed to the dryer.

The initial conditions are found by converting the initial condition of Eq. 12, $f(x|0) = M_T(0)\delta(x - x^0)$ to

$$g(z|0) = \delta(z)$$

$$\mu_0(0) = 1$$

$$\mu_1(0) = 0$$

Now equations can be defined for $\mu_0(\theta)$ and $\mu_1(\theta)$ that do not require $g(z|\theta)$:

Initial interval ($0 \leq \theta < 1$)

$$\mu_0(\theta) = 1 + \int_0^\theta \alpha(v)\mu_0(v)\,dv \tag{34a}$$

$$\frac{d\mu_0(\theta)}{d\theta} = \alpha(\theta)\mu_0(\theta) \tag{34b}$$

$$\mu_1(\theta) = \theta + \int_0^\theta (\theta - v)\alpha(v)\mu_0(v)\,dv \tag{35a}$$

$$\frac{d\mu_1(\theta)}{d\theta} = \mu_0(\theta) \tag{35b}$$

General case ($\theta \geq 1$)

$$\mu_0(\theta) = \int_{\theta-1}^\theta \alpha(v)\mu_0(v)dv \tag{36a}$$

$$\frac{d\mu_0(\theta)}{d\theta} = \alpha(\theta)\mu_0(\theta) - \alpha(\theta - 1)\mu_0(\theta - 1) \tag{36b}$$

$$\mu_1(\theta) = \int_{\theta-1}^\theta (\theta - v)\alpha(v)\mu_0(v)dv \tag{37a}$$

$$\frac{d\mu_1(\theta)}{d\theta} = \mu_0(\theta) - \alpha(\theta - 1)\mu_0(\theta - 1) \tag{37b}$$

Obtaining expressions for time, t, and total amount of solid in dryer, M_T, as a function of θ

Expressing μ_0 and μ_1 as a function of θ is very useful when solving the corresponding equations numerically in the next section. However, dimensionless time θ is not a practical variable when operating dryers and interpreting results. Therefore, it is converted to actual time t by rewriting Eq. 19

$$\frac{dt}{d\theta} = \alpha(0)\mu_0(\theta)\tau_0 \tag{38}$$

where $\tau_0 = M_T(0)/w^0(0)$.

The end of process time, t_{end}, is calculated using the mass balance (see Appendix). The total amount of solid in the dryer is calculated using Eq. 3 (with constant χ)

$$\frac{dM_T(\theta)}{d\theta} = \alpha(\theta)\mu_0(\theta)M_T(0) \tag{39}$$

This section and the previous section have shown that $g(z|\theta)$, $\mu_0(\theta)$, $\mu_1(\theta)$, $t(\theta)$, and $M_T(t)$ can all be written in terms of $\mu_0(\theta)$ and α. Solving the ODE of $\mu_0(\theta)$ enables solution of all presented ODEs. This is performed using a numerical solution strategy presented in the next section.

Numerical Solution of $\mu_0(\theta)$ and $\mu_1(\theta)$

The ODEs derived in the previous section can be solved by dividing θ into $n\theta$ segments of length 1 and introducing a local version of θ for each segment, θ'. In each ith segment functions based on this local drying extent can be defined. In

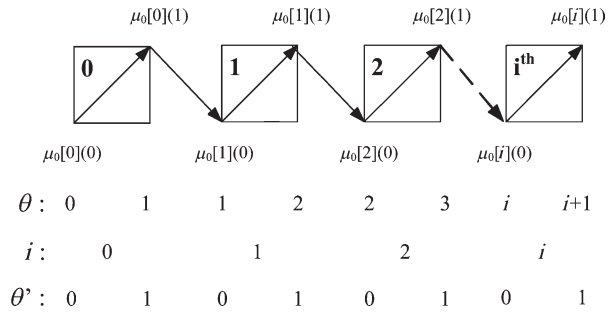

Figure 4. Piecewise solution of $\mu_0(\theta)$ by dividing θ into $n\theta$ segments. ODEs for μ_0, μ_1, and t are solved for θ' in each ith segment and combined to obtain the solution over θ.

The stepsize of each segment is 1. Solution is obtained by differentiating within each segment from $\theta' = 0$ to $\theta' = 1$. It is emphasized that $\mu_0[0](1) = \mu_0[1](0)$.

the annotations, the square brackets represent the segment number, and the parentheses give the value of the variable θ'.

$$\mu_0[i](\theta') = \mu_0(\theta) \tag{40}$$

$$\mu_1[i](\theta') = \mu_1(\theta) \tag{41}$$

$$\alpha[i](\theta') = \alpha(t[i](\theta')) \tag{42}$$

$$t[i](\theta') = t(\theta) \tag{43}$$

where $\theta' = \theta - i$. The length of a segment i is 1, which implies that the values of θ' are between 0 and 1 (0 being the initial value and 1 the end value within a segment). The solution strategy to find $\mu_0(\theta)$ and $\mu_1(\theta)$ is based on an evolutionary progression of local solutions where the output of one segment (i.e., $\theta'[i-1] = 1$) is the input of the subsequent segment (i.e., $\theta'[i] = 0$). Figure 4 presents a schematic presentation of this segmentation technique for $\mu_0(\theta)$. Equations 34b, 35b, 36b, 37b, and 38 can now be solved numerically for each segment (i.e., $i = 0 \ldots n\theta$).

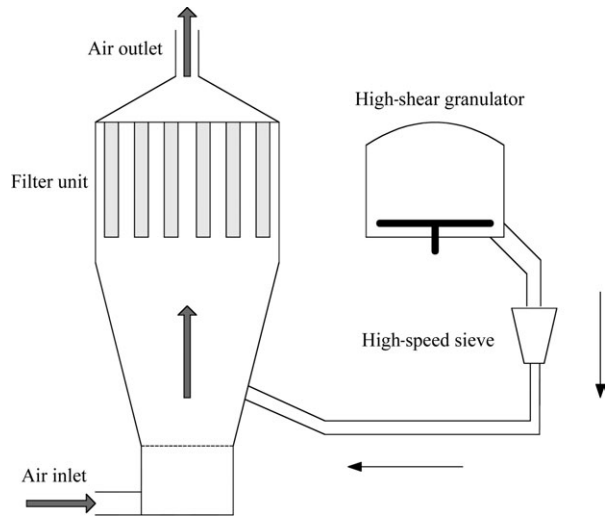

Figure 5. Schematic overview of a semibatch fluidized bed drying process.

Wet granules are pneumatically fed from the high-shear granulator, optionally via a high-speed sieve, to the fluidized bed. The large gray arrows mark the direction of the airflow inside the fluidized bed.

$i = 0$: first interval ($0 \le \theta < 1$)

For $i = 0$, Eqs. 34b and 35b become

$$\frac{d\mu_0[0](\theta')}{d\theta'} = \alpha[0](\theta')\mu_0[0](\theta') \quad (0 \le \theta < 1) \tag{44a}$$

$$\frac{d\mu_1[0](\theta')}{d\theta'} = \mu_0[0](\theta') \quad (0 \le \theta < 1) \tag{44b}$$

with initial conditions $\mu_0[0](0) = 1$ and $\mu_1[0](0) = 0$.

$i = 1$: second interval ($1 \le \theta < 2$)

From Eqs. 36b and 37b, it would be expected that for $\theta \ge 1$ a general set of equations could be defined. However, it has to be taken into account that at $\theta = 1$ there is a discontinuity in the dimensionless mass of wet particles $\mu_0(\theta)$. At this point, $z = 1$ for the initial charge of wet particles, which means that they leave the wet particles population and join the dry population $M_T^*(t)$. This implies that the initial condition at $i = 1$ for $\mu_0(\theta)$ and $\mu_1(\theta)$ becomes

$$\mu_0[1](0) = \mu_0[0](1) - 1$$
$$\mu_1[1](0) = \mu_1[0](1) - 1$$

where 1 represents the normalized initial charge of wet particles. Equations 36b and 37b are solved numerically using these initial conditions and the following equations

$$\frac{d\mu_0[1](\theta')}{d\theta'} = \alpha[1](\theta')\mu_0[1](\theta') - \alpha[0](\theta')\mu_0[0](\theta') \quad (1 \le \theta < 2) \tag{45a}$$

$$\frac{d\mu_1[1](\theta')}{d\theta'} = \mu_0[1](\theta') - \alpha[0](\theta')\mu_0[0](\theta') \quad (1 \le \theta < 2) \tag{45b}$$

$i > 2$: general case for subsequent intervals ($\theta \ge 2$)

For the general case, the initial condition $\mu_0[i](0)$ is obtained from the final condition $\mu_0[i-1](1)$ without the requirement to correct for the initial charge, that is, $\mu_0[i](0) = \mu_0[i-1](1)$. This means that the following set of equations is applicable for these intervals

$$\frac{d\mu_0[i](\theta')}{d\theta'} = \alpha[i](\theta')\mu_0[i](\theta') - \alpha[i-1](\theta')\mu_0[i-1](\theta') \quad (\theta \ge 2) \tag{46a}$$

$$\frac{d\mu_1[i](\theta')}{d\theta'} = \mu_0[i](\theta') - \alpha[i-1](\theta')\mu_0[i-1](\theta') \quad (\theta \ge 2) \tag{46b}$$

General solution for time t and total amount of solid $M_T(t)$

Equations 38 and 39, describing, respectively, time and total amount of solid in the dryer as a function of θ', can also be solved using this numerical approach. However, no distinction between different intervals is required for these variables, as they are not related to moisture content x and,

Table 1. Calculated α Values for Different Operating Settings of Drying Rate (χ) and Feed Rate (w^0)

χ (kg/s)	0.0025	0.00375	0.005
$w^0 = 0.067$ kg/s	2.667	1.778	1.333
$w^0 = 0.100$ kg/s	4.000	2.667	2.000

Table 2. Input Parameters That were Kept Constant During Simulation Experiments

Parameter	Setting
Initial mass of wet granules ($M_T(0)$)	1 kg dry solid
Total batch loading (M_{total})	100 kg dry solid
Initial moisture content (x^0)	0.15 kg H_2O/kg dry solid
Final moisture content (x^*)	0.05 kg H_2O/kg dry solid

therefore, do not have to be divided into wet and dry populations. Equations 38 and 39 are rewritten numerically as

$$\frac{dt[i](\theta')}{d\theta'} = \alpha[0](0)\mu_0[i](\theta')\tau_0 \tag{47}$$

$$\frac{dM_T[i](\theta')}{d\theta'} = \alpha[i](\theta')\mu_0[i](\theta') \tag{48}$$

with initial conditions $t[0](0) = 0$ and $M_T[0](0) = 1$.

Finding g(z|θ), f(x|t) and the overall average moisture content $\bar{x}_{overall}(t)$

The dimensionless moisture content distribution, $g(z|\theta)$, is calculated using Eqs. 32 and 33:

$$g(z|\theta) = \alpha(\theta - z)\mu_0(\theta - z) \tag{49}$$

$g(z|\theta)$ is converted to the moisture content distribution of wet particles in the dryer $f(x|t)$ using Eq. 23. $m_0(t)$ is obtained from $\mu_0(\theta)$ by multiplying the latter with $M_T(0)$ (see Eq. 26). $m_1(t)$ is obtained from $\mu_1(\theta)$ using Eqs. 18, 22, and 28

$$m_1(t) = \left(\mu_1(\theta) + \frac{x^0}{x^* - x^0}\mu_0(\theta)\right)M_T(0)(x^* - x^0) \tag{50}$$

Equations 15–17 have shown how $m_0(t)$ and $m_1(t)$ can be used to obtain the overall moisture content, $\bar{x}_{overall}(t)$ and the fraction of dry particles.

"Mathematica" provides a convenient environment to solve these equations. The appendix contains the Mathematica code fragments to solve the ODEs. The next section shows how this model can be applied using a semibatch fluidized bed drying process as an example.

Simulation Studies

Input values for simulation

In this section, the model and solution strategy presented in the previous section are applied to a hypothetical semibatch fluidized bed drying process (see Figure 5). The fluidized bed is pneumatically fed with agglomerated primary particles that will be named granules in this section. When these granules enter the dryer, they contain a moisture content x^0. Other input values for feed rate, w^0, total batch loading, M_{total}, and drying rate, χ, were derived from practice. Simulation experiments were performed at two different feed rates: 0.067 and 0.100 kg/s. At each feed rate, χ was varied at three levels: 0.0025, 0.00375, and 0.005 kg/s. This results in different values for α (see Table 1). Table 2 shows the parameters that were kept constant throughout all simulations.

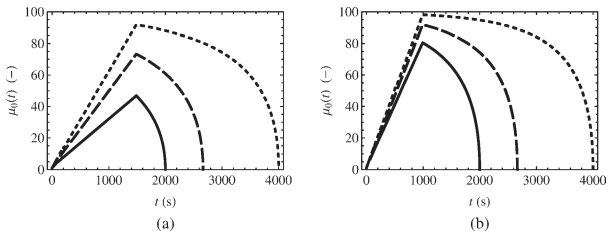

Figure 6. Dimensionless mass of wet granules, μ_0, as a function of time, *t*.

Two feed rates are presented: 0.067 kg/s (a) and 0.100 kg/s (b). In each graph, three drying rates are presented: 0.0025 kg/s (···), 0.00375 kg/s (- - -), and 0.005 kg/s (—).

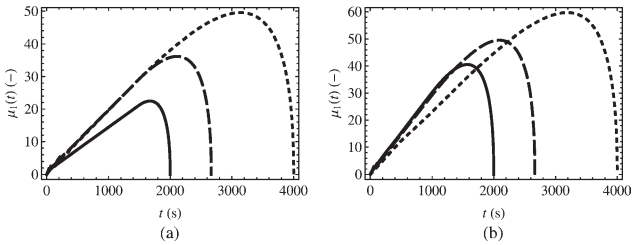

Figure 7. Dimensionless mass of dryness among wet granules, μ_1, as a function of time, *t*.

Two feed rates are presented: 0.067 kg/s (a) and 0.100 kg/s (b). In each graph, three drying rates are presented: 0.0025 kg/s (···), 0.00375 kg/s (- - -), and 0.005 kg/s (—).

Results and Discussion

Solution of Eqs. 34b and 35b using the strategy presented in the previous section gives μ_0 and μ_1 as a function of θ. Conversion into actual time t using Eq. 38 results in Figure 6. Figure 6 shows that a higher drying rate χ results in a slower increase of the amount of wet granules represented by $\mu_0(t)$. This is explained by the definition of $\mu_0(t)$. $\mu_0(t)$ only includes the dimensionless mass of wet granules, that is no dry granules are included in these graphs. A higher drying rate results in a higher amount of granules joining the dry granule population per unit of time and thus a relatively smaller amount of wet granules. Therefore, higher drying rates result in lower values for $\mu_0(t)$.

Figure 6 also shows that an increase of feed rate from 0.067 to 0.100 kg/s using the same drying rate of 0.005 kg/s gives relatively more wet granules than a drying rate of 0.0025 kg/s. At 0.005 kg/s, the rate of granules joining the dry population in the dryer is smaller than the rate of wet granules entering the dryer. At 0.0025 kg/s, the amount of granules joining the dry granule population is already small.

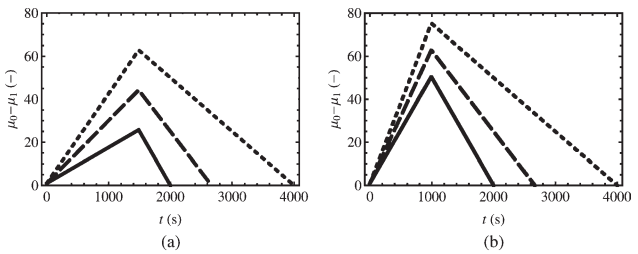

Figure 8. Total dimensionless wetness among wet granules, ($\mu_0 - \mu_1$) as a function of time (in seconds).

Two feedrates are presented: 0.067 kg/s (a) and 0.100 kg/s (b). In each graph, three drying rates are presented: 0.0025 kg/s (···), 0.00375 kg/s (- - -), and 0.005 kg/s (—).

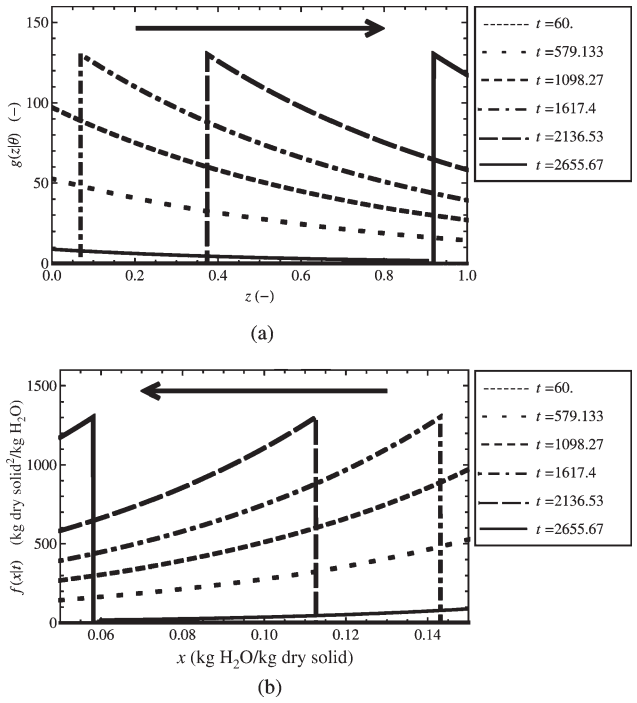

Figure 9. Evolution in absolute time *t* of dimensionless particle density distribution of *g*(*z*|θ) as a function of dimensionless dryness *z* (a) and mass density distribution *f*(*x*|*t*) as a function of *x* (b).

Feed rate, w^0, is 0.067 kg/s. Drying rate, χ, is 0.00375 kg/s. Solid line of $t = 0$ is plotted on the *x*-axis. The arrows show the general direction of movement in time *t*.

Therefore, an increase of feed rate has a less significant effect.

The difference in end of process time t_{end} is caused by differences in drying rate. A higher drying rate gives a faster rate of granules joining the dry granule population and, therefore, a shorter end of process time. This is also shown in Eq. 51. The total process times of both feed rates are similar for every drying rate. This similarity is caused by the assumption that drying rate, χ, and feed rate, w^0, are constant. Both parameters are included in α (see Eq. 25). The end of process time, defined in the Appendix, is a function of α and total feeding time (see Eq. A7). For this drying process (i.e., with one feeding step), Eq. A7 can be rewritten as

Figure 10. Mass density function *f*(*x*|*t*) (kg dry solid^2 kg H_2O^{-1}) as a function of *x* at the end of feeding.

Two feed rates are presented: 0.067 kg/s (a) and 0.100 kg/s (b). In each graph, three drying rates are presented: 0.0025 kg/s (···), 0.00375 kg/s (- - -), and 0.005 kg/s (—).

$$t_{end} = \frac{(x^0 - x^*)(M_T(0) + M_{feed})}{\chi} \tag{51}$$

where $M_{feed} = M_{total} - M_T(0)$.

Equation 51 shows that the end of process time is independent of w^0, which is consistent with the observation in Figure 6. Figure 6 reveals a linear relationship between μ_0 and t during feeding. This relationship is not explained here but will be discussed in more detail in a forthcoming article. Figure 7 shows the mass of dryness among wet granules, μ_1 as a function of t. Intuitively, it would be expected that a higher drying rate would result in a higher value for $\mu_1(t)$. Figure 7a shows that for drying rates 0.00375 and 0.005 kg/s, the increase of $\mu_1(t)$ is similar and the slowest drying rate, 0.0025 kg/s, the increase of $\mu_1(t)$ is smaller. However, Figure 7a shows that 0.0025 and 0.00375 kg/s, the increase of $\mu_1(t)$ is similar and the slowest drying rate, 0.005 kg/s, the increase of $\mu_1(t)$ is smaller. Here, the same explanation applies as for $\mu_0(t)$. $\mu_1(t)$ represents the mass of dryness among wet granules. Thus, dry granules are not included. For the higher drying rate $\chi = 0.005$ kg/s, more granules have already joined the dry granule population and, therefore, are not included in $\mu_1(t)$. For $\mu_1(t)$ to be calculated, wet granules have to be present in the dryer. More wet granules mean more mass of dryness. Hence, $\mu_1(t)$ is higher for lower drying rates, especially at higher feed rates.

This is shown even better when plotting the dimensionless wetness. The dimensionless wetness as a function of t is obtained using Eq. 38 to convert Eq. 31 to

$$\frac{d(\mu_0(t) - \mu_1(t))}{dt} = \frac{\alpha(t) - 1}{\alpha(0)\tau_0} \tag{52}$$

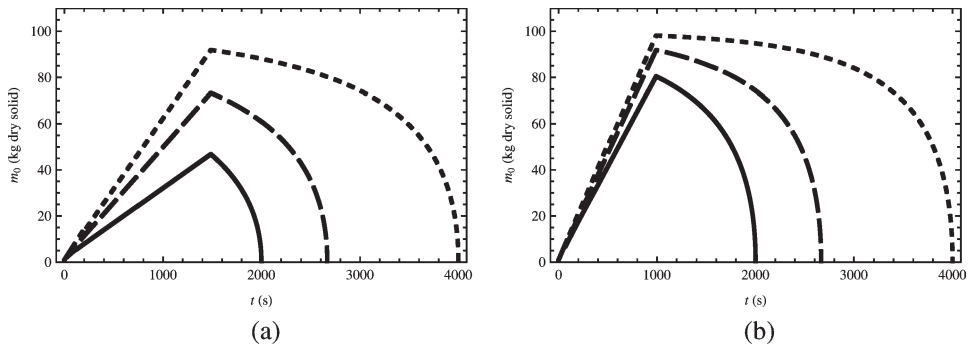

Figure 11. Mass of wet granules in dryer, m_0 (in kg dry solid), as a function of time *t*.

Two feed rates are presented: 0.067 kg/s (a) and 0.100 kg/s (b). In each graph, three drying rates are presented: 0.0025 kg/s (···), 0.00375 kg/s (- - -), and 0.005 kg/s (—).

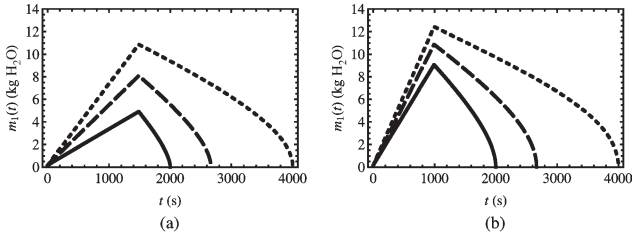

Figure 12. Total mass of moisture in wet granules, m_1 (in kg H_2O), as a function of time t.

Two feed rates are presented: 0.067 kg/s (a) and 0.100 kg/s (b). In each graph, three drying rates are presented: 0.0025 kg/s (···), 0.00375 kg/s (- - -), and 0.005 kg/s (—).

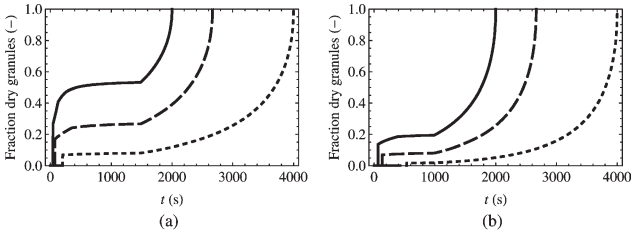

Figure 14. The fraction of dry granules in the fluidized bed dryer as a function of time (in seconds).

The fraction of dry granules is calculated from $m_0(t)$ and $M_T(t)$ using Eq. 16. Two feed rates are presented: 0.067 kg/s (a) and 0.100 kg/s (b). In each graph, three drying rates are presented: 0.0025 kg/s (···), 0.00375 kg/s (- - -), and 0.005 kg/s (—).

where during feeding: $\alpha(t) = \alpha\ (0)$ and after feeding: $\alpha(t) = 0$

When plotting $(\mu_0 - \mu_1)$ as a function of time t, a straight line with slope $(\alpha(0) - 1)/\alpha(0)$ for $t \leq t_f$ and a second straight line for $t > t_f$ with a slope of $-1/(\alpha(0)\tau_0)$ should be obtained (see Figure 8). Figure 8 shows that for a feed rate of 0.100 kg/s during the feeding phase, the total wetness per unit of time of all drying rates increases compared to a feed rate of 0.067 kg/s. This increase is more significant for a higher drying rate than a lower drying rate and can be explained by the same explanation as for $\mu_0(\theta)$, namely a higher amount of granules joining the dry granule population for higher drying rates (see also Figure 14).

Using $\mu_0(\theta)$ and $\alpha(\theta)$, the dimensionless moisture content distribution, $g(z|\theta)$, is calculated using Eqs. 32 and 33. Figure 9a illustrates how $g(z|\theta)$ as a function of z evolves in time for feed rate 0.067 kg/s and drying rate 0.005 kg/s. $g(z|\theta)$ is easily converted into the moisture content distribution of wet granules in the fluidized bed dryer, $f(x|t)$, using Eq. 23. Figure 9b shows $f(x|t)$ as a function of t. The sharp decrease observed in both figures is caused by discontinuation of the inlet stream, w^0, that is, no new wet granules are fed to the dryer. Figure 10 shows the moisture content distribution of wet granules in the dryer at the end of feeding. A feed rate of 0.100 kg/s results, especially in the higher region of x ($x > 0.10$), in a higher amount of wet granules for all drying rates. This means that more solvent has to be removed in the drying phase compared to a feed rate of 0.067 kg/s.

The area under the curve of $f(x|t)$ is defined as $m_0(t)$ (see Eq. 13), which is the total mass of wet granules in the dryer. $m_0(t)$ is obtained using Eq. 26 and is shown in Figure 11.

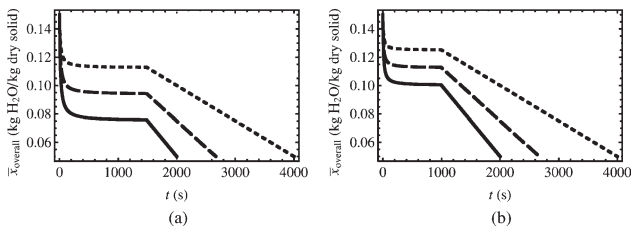

Figure 13. Overall average moisture content, $\bar{x}_{overall}$ (in kg H_2O/kg dry solid) in the fluidized bed dryer as a function of time (in seconds).

The fraction of dry granules was calculated from p_{dry} and $\bar{x}$ using Eq. 17. Two feed rates are presented: 0.067 kg/s (a) and 0.100 kg/s (b). In each graph, three drying rates are presented: 0.0025 kg/s (···), 0.00375 kg/s (- - -), 0.005 kg/s (—).

Figure 11 is very similar to Figure 6 as $M_T(0)$ in Eq. 26 is 1 kg dry solid (see Table 2).

Figure 12 shows m_1 as a function of time t. The same patterns can be observed as for $m_0(t)$. A higher feed rate results in a higher total amount of solvent in wet granules. The average moisture content of wet granules, $\bar{x}(t)$, is obtained from: $m_1(t)/m_0(t)$ (see Eq. 15. Control of drying processes is often performed on the basis of average properties. The overall average moisture content, $\bar{x}_{overall}(t)$, in the fluidized bed dryer is a parameter that is often used for this purpose (e.g. using near infrared spectroscopy). Values for $\bar{x}_{overall}(t)$ are calculated using Eq. 17. Figure 13 shows the results of both feed rates. Comparing Figures 13a, b illustrates the dependence of drying time on drying rate and feed rate. A higher feed rate results in a longer drying time and a higher drying rate gives a shorter drying time when using a similar feed rate. Furthermore, it can be observed that during feeding after a fast decrease of moisture content, the moisture content reaches a plateau value. This will be explained in more detail in a forthcoming article.

The model presented in this article also provides additional parameters for process monitoring and control. An example is evolution of the fraction of dry granules. Equation 16 gives the fraction of dry granules in the fluidized bed dryer. This fraction should be 1 at $t = t_{end}$, that is, all granules have a moisture content that corresponds to the equilibrium moisture content, x^*. Figure 14 shows the results for different feed rates and drying rates. Feed rate has the most influence on the highest drying rate (i.e., 0.005 kg/s). After feeding, a feed rate of 0.067 kg/s gives a fraction of dry granules of $\sim$0.5 for this drying rate, whereas for a feed rate of 0.100 kg/s this fraction is $\sim$0.2. This difference is much smaller for lower drying rates.

Conclusions

From the simulation results, it is concluded that the model and solution strategy presented in this article give a feasible interpretation of a semibatch drying process. Some characteristic results (plateau-values for $\bar{x}_{overall}(t)$ during feeding and linear relationship of μ_0 vs. t during feeding) have not been discussed but will be explained in a forthcoming article.

The model not only gives the evolution of overall moisture content in time, but also shows how the moisture content distribution changed within a population of wet particles during feeding and drying. This is a powerful insight that can be used to design drying processes for materials with specifications for individual particle

moisture contents. The model also allows flexibility to use different key control parameters, for example, number of feeding phases, drying rate, feed rate, and total batch loading. Moreover, it is not directly coupled to heat and mass transfer equations making it flexible to apply in different environments.

The authors acknowledge that the assumption of constant particle drying rate is not always valid in real systems. Therefore, in a forthcoming article, this model will be extended to falling particle drying rate.[12] Once these models have been validated experimentally, they can be used to develop industrial drying processes more efficiently (e.g., as part of the "Quality by Design" approach in pharmaceutical industry) or extended further to model predictive control of drying processes.

Acknowledgment

The authors thank Jellis Knöps for making his MEng thesis available for reading.

Literature Cited

1. Chandran AN, Subba Rao S, Varma YBG. Fluidized bed drying of solids. *AIChE J*. 1990;36(1):29–38.
2. Burgschweiger J, Tsotsas E. Experimental investigation and modelling of continuous fluidized bed drying under steady state and dynamic conditions. *Chem Eng Sci*. 2002;57:5021–5038.
3. Burgschweiger J, Groenewold H, Hirschmann C, and Tsotsas E. From hygroscopic single particle to batch fluidized bed drying kinetics. *Can J Chem Eng*. 1999;77(2):333–341.
4. Heinrich S, Peglow M, Tsotsas E, Mörl L. Fluidized bed drying: influence of dispersion and transport phenomena, Vol. A. In: Proceedings of the 14th International Drying Symposium (IDS2004). Sao Paulo, Brazil, 2004:129–136
5. Wang HG, Dyakowski T, Senior P, Raghavan RS, Yang WQ. Modelling of batch fluidized bed drying of pharmaceutical granules. *Chem Eng Sci*. 2007;62(5)1524–1535.
6. Mihálykó Cs, Lakatos BG, Matejdesz A, Blickle T. Population balance model for particle-to-particle heat transfer in gas–solid systems. *Int J Heat Mass Transfer*. Elsevier Science, Amsterdam, The Netherlands, 2004;47:1325–1334.
7. Süle Z, Mihálykó Cs, Lakatos BG. Modeling of heat transfer processes in particulate systems. In: *16th European Symposium on Computer Aided Process Engineering and 9th International Symposium on Process Systems Engineering*. 2006:589–594.
8. Syahrul S, Hamdullahpur F, Dincer I. Thermal analysis in fluidized bed drying of moist particles. *Appl Therm Eng*. 2002;22:1763–1775.
9. Metzger T, Kwapinska M, Peglow M, Saage G, Tsotsas E. Modern modelling methods in drying. *Transp Porous Media*. 2007;66:103–120.
10. Peglow M, Cunäus U, Tsotsas E. An analytical solution of population balance equations for continuous fluidized bed drying. *Chem Eng Sci*. 2011;66:1916–1922.
11. Strumillo C, Kudra T. *Drying: Principles, Applications and Design*. Montreax: Gordon and Breach Science Publishers, 1986.
12. Nitert BJ, Hounslow MJ. Moisture content distribution in semi-batch drying processes: part 2: falling particle drying rate. *AIChE J*. In press.

Appendix

Obtaining an expression for t_{end}

The feed rate of wet granules, w^0, can change with time. For example, three phases can be distinguished: feeding phase 1, feeding phase 2, and drying phase. For both feeding phases, different feed rates apply. This appendix shows how the end of process time, t_{end}, can be calculated from a changing α. The assumption is made that α is constant during a feeding phase. The following expression applies

$$\int_0^{t_{end}} \chi\, dt = M_T(0)(x^0 - x^*) + \int_0^{t_{end}} w^0(t)(x^0 - x^*)\, dt \quad \text{(A1)}$$

Integrating the LHS

$$\chi \cdot t_{end} = M_T(0)(x^0 - x^*) + \int_0^{t_{end}} w^0(t)(x^0 - x^*)\, dt \quad \text{(A2)}$$

Dividing by $\chi(t) \cdot t_{end}$ and substituting Eq. 25:

$$1 = \frac{M_T(0)(x^0 - x^*)}{\chi \cdot t_{end}} + \frac{1}{t_{end}} \int_0^{t_{end}} \alpha(t)\, dt \quad \text{(A3)}$$

The first part of RHS can be written as

$$\frac{M_T(0)(x^0 - x^*)}{\chi} = \frac{M_T(0)}{w^0(0)} \cdot \frac{w^0(0)(x^0 - x^*)}{\chi} = \alpha(0)\tau_0 \quad \text{(A4)}$$

where $\tau_0 = M_T(0)/w^0(0)$.

Substituting Eq. A4 into Eq. A3 gives

$$\frac{t_{end}}{\tau_0} = \alpha(0) + \frac{1}{\tau_0} \int_0^{t_{end}} \alpha(t)\, dt \quad \text{(A5)}$$

$$t_{end} = \alpha(0)\tau_0 + \int_0^{t_{end}} \alpha(t)\, dt \quad \text{(A6)}$$

This gives after stepwise integration for t_{end}

$$t_{end} = \alpha(0)\tau_0 + \alpha(t_{f,1})t_{f,1} + \alpha(t_{f,2})t_{f,2} + \alpha(t_{dry})t_{dry} \quad \text{(A7)}$$

$$= \alpha(0)\tau_0 + \alpha(t_{f,1})t_{f,1} + \alpha(t_{f,2})t_{f,2} \quad \text{(A8)}$$

where $t_{f,1}$ is the time of feeding phase 1, $t_{f,2}$ is the time of feeding phase 2, and t_{dry} is the drying time after feeding. The total feed time is the sum of $t_{f,1}$ and $t_{f,2}$. The term $\alpha(t_{dry})t_{dry}$ is zero, as there is no feeding during this phase (see definition of α, Eq. 25). With this last equation, the process end time can be calculated and incorporated into the piecewise solution strategy of μ_0 and μ_1. The total feeding time (t_f) is obtained from $(M_{total} - M_T(0))/w^0$.

In this article, the process consists of one feeding step, that is, the part including $t_{f,2}$ in Eq. A7 was deleted. However, for simulations with multiple feeding steps, Eq. A7 can be easily extended to include different feed phases.

Mathematica code fragments

In this appendix the Mathematica code fragments for the piecewise solution of Eqs. 44a–47 are presented. Here, "totalsolid" is the total amount of wet granules fed to the dryer and "M0" is the initial charge (in kg).

μ_0 and time t

```
eq[0] =  {μ0[0][θ] == α[t[0][θ]]μ0[0][θ], μ0[0][0] == 1,
          t[0][θ] == α[0]μ0[0][θ]tau0, t[0][0] == 0}

eq[1] =  {μ0[1][θ] == α[t[1][θ]]μ0[1][θ] − α[nt[0][θ]]nμ0[0][θ],
          μ0[1][0] == nμ0[0][1] − 1,
          t[1][θ] == α[0]μ0[1][θ]tau0,    t[1][0] == nt[0][1]}
```

```
eq[i_] := {μ0[i][θ] == α[t[i][θ]]μ0[i][θ] − α[nt[i − 1][θ]]nμ0[i − 1][θ],
           μ0[i][0] == nμ0[i − 1][1],
           t[i][θ] == α[0]μ0[i][θ]tau0,  t[i][0] == nt[i − 1][1]}/; i > 1

Do[sol =   NDSolve[eq[i], {μ0]i], t]i]}, {θ, 0, 1}][[1]];
           nμ0[i] = μ0[i]/.sol;
           nt[i] = t[i]/.sol, {i, 0, nθ}]

moment0[θ_] := n μ 0[IntegerPart[θ]][FractionalPart[θ]]
time[θ_] := nt[IntegerPart[θ]][FractionalPart[θ]]
```

μ_1, total mass of solid (on dry basis) and g(z/θ)

```
eq1[0] = {μ1[0][θ] == nμ0[0][θ],  μ1[0][0] == 0,
          M[0][θ] == α[nt[0][θ]]nμ0[0][θ],  M[0][0] == 1}

eq1[1] = {μ1[1][θ] == nμ0[1][θ] − α[nt[0][θ]]nμ0[0][θ],
          μ1[1][0] == nμ1[0][1] − 1,
          M[1], [θ] == α[nt[1][θ]]nμ0[1][θ],
               M[1][0] == nM[0][1]}

eq1[i_] := {μ1[i][θ] == nμ0[i][θ] − α[nt[i − 1][θ]]nμ0[i − 1][θ],
            μ1[i][0] == nμ0[i − 1][1],
            M[i][θ] == α[nt[i][θ]]nμ0[i][θ],
            M[i][0] == nM[i − 1][1]}/; i > 1

Do[sol = NDSolve[eq[i], {μ1]i], M]i]}, {θ, 0, 1}][[1]];
           nμ1[i] = μ1[i]/.sol;
           nM[i] = M[i]/.sol, {i, 0, nθ}]

moment1[θ_] := n μ 1[IntegerPart[θ]][FractionalPart[θ]]
totalsolid[θ_] := nM[IntegerPart[θ]][FractionalPart[θ]] M0

g[z_, θ_] := α [time[θ − z]] moment0[θ − z]/; θ >= z
g[z_, θ_] := 0 /; θ < z
f[x_, t_] := M0/Abs[xeq − x0] g[z[x], θ oft[t]]
```

where "θoft" is obtained from a bracketing routine.

Manuscript received Jun. 25, 2011, revision received Dec. 28, 2011, and final revision received Mar. 6, 2012.